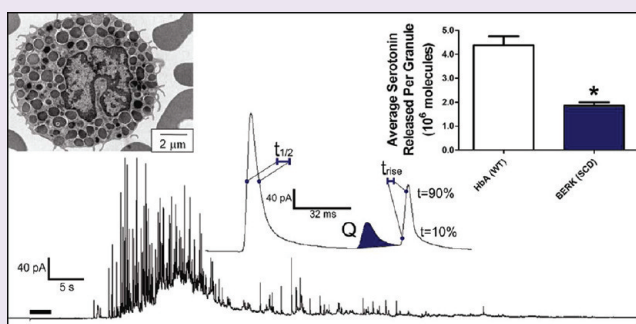


Carbon-Fiber Microelectrode Amperometry Reveals Sick-Cell-Induced Inflammation and Chronic Morphine Effects on Single Mast Cells

Benjamin M. Manning,[†] Robert P. Hebbel,[‡] Kalpna Gupta,[‡] and Christy L. Haynes^{†,*}

[†]Department of Chemistry and [‡]Vascular Biology Center, Division of Hematology, Oncology & Transplantation, Department of Medicine, University of Minnesota, Minneapolis, Minnesota 55455, United States

ABSTRACT: Sick cell disease, caused by a mutation of hemoglobin, is characterized by a complex pathophysiology including an important inflammatory component. Mast cells are tissue-resident leukocytes known to influence a range of immune functions in a variety of different ways, largely through the secretion of biologically active mediators from preformed granules. However, it is not understood how mast cells influence the inflammatory environment in sickle cell disease. A notable consequence of sickle cell disease is severe pain. Therefore, morphine is often used to treat this disease. Because mast cells express opioid receptors, it is pertinent to understand how chronic morphine exposure influences mast cell function and inflammation in sickle cell disease. Herein, carbon-fiber microelectrode amperometry (CFMA) was used to monitor the secretion of immunoactive mediators from single mast cells. CFMA enabled the detection and quantification of discrete exocytotic events from single mast cells. Mast cells from two transgenic mouse models expressing human sickle hemoglobin (hBERK1 and BERK) and a control mouse expressing normal human hemoglobin (HbA-BERK) were monitored using CFMA to explore the impact of sickle-cell-induced inflammation and chronic morphine exposure on mast cell function. This work, utilizing the unique mechanistic perspective provided by CFMA, describes how mast cell function is significantly altered in hBERK1 and BERK mice, including decreased serotonin released compared to HbA-BERK controls. Furthermore, morphine was shown to significantly increase the serotonin released from HbA-BERK mast cells and demonstrated the capacity to reverse the observed sickle-cell-induced changes in mast cell function.



Sickle cell disease (SCD) became the first recognized “molecular disease” when Linus Pauling discovered the altered electrophoretic mobility of hemoglobin (Hb) in the blood of patients suffering from this painful and often life-threatening disorder.¹ Several years later, the genetic basis for the dysfunctional Hb was determined.^{2,3} However, despite its simple origin, the pathophysiology of this disease is complex and highly variable,³ and relatively few advances in treatment methods have been made. A large part of the diverse manifestation of SCD can be attributed to the significant inflammatory component of the disease.^{4–7} Understanding the specific role of inflammation in the development and progression of SCD requires a capacity to monitor the behavior of different cell types that take part in the inflammatory response. In addition to traditional molecular biology methods such as bulk *in vitro* assays to detect various secreted mediators or immunostaining to observe relative levels of immune cell infiltrate *in situ*, single cell measurement techniques can provide a complementary approach to study fundamental cellular functions of the immune system. Understanding how mast cells respond to the chronic inflammation associated with SCD provides an interesting and important perspective on its pathophysiology and progression.

Carbon-fiber microelectrode amperometry (CFMA) is a unique analytical tool for the real-time, label-free detection of secreted molecular species from single cells.⁸ Single cell electrochemical measurements correlate well with both single vesicle measurements and bulk assays.^{9,10} In this case, CFMA can be used to measure from single mast cells¹¹ based on the high spatial resolution of these electrodes and the high sensitivity and low background current achieved. CFMA measurements are conducted by holding the microelectrode, placed in contact with a single cell, at a fixed potential sufficient to oxidize the molecular species of interest (Figure 1A–C). Upon stimulation, distinct packets of current are detected as oxidizable species are released from each granule of the cell (Figure 1D). The ability to quantitatively measure individual exocytosis events from these cells offers a useful handle on the various physiological functions mast cells perform within the immune system.

Because they influence a variety of immune responses,^{12–14} mast cells are subsequently implicated in many inflammatory

Received: September 7, 2011

Accepted: January 4, 2012

Published: January 4, 2012

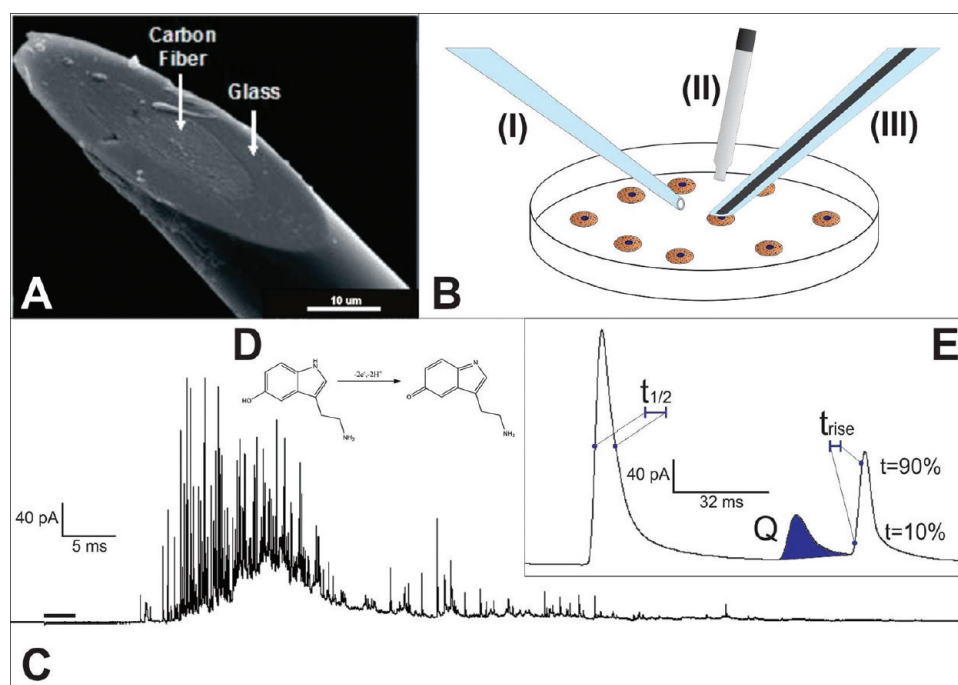


Figure 1. Carbon-fiber microelectrodes (A) were polished to a 45° angle with an active surface of roughly 10 μm in diameter. The CFMA experimental setup (B) included (I) a pulled glass stimulating pipet, (II) a Ag/AgCl reference electrode, and (III) the carbon-fiber microelectrode set to an oxidizing potential and placed in contact with a single mast cell. Amperometric traces (C) were collected as current was detected when serotonin was released to the exterior of the cell and oxidized (D) at the surface of the microelectrode. Individual current spikes were analyzed (E) for several parameters including spike area (Q), spike half-width ($t_{1/2}$), spike rise-time (t_{rise}), and spike frequency.

diseases. SCD is one such example, and because it is painful, patients are often treated with opioids such as morphine.^{15–17} One common side effect of morphine treatment is severe itching and reddening, indicating unintentional activation of mast cells, likely exacerbating the pain symptoms.¹⁸ Morphine-mediated mast cell degranulation is poorly understood, and because it occurs at much higher doses than are used for pain management, it is thought to function independent of opioid receptors.^{18–20} Herein, CFMA is used to, first, explore the impact of sickle Hb expression and the subsequent inflammation on mast cell function, and, second, gain biophysical insight into the effect of chronic morphine exposure on mast cell degranulation dynamics at the single cell level. Furthermore, the effect of morphine on mast cell function is also examined in the context of sickle Hb-induced inflammation.

Mast cells are granulated leukocytes of hematopoietic origin that circulate in the peripheral blood as progenitors before migrating to connective tissues throughout the body where they undergo final maturation.^{13,21} Mast cells are often located proximal to blood vessels and mucosal surfaces, suggesting an important role in the innate immune system.^{13,22} The dominant feature of mast cells is the dense-body secretory granules found throughout their cytoplasm (Figure 2A). These granules store many mediators that influence the inflammatory response. Secretion of these mediators *via* exocytosis (Figure 2B) can be triggered by several signaling mechanisms. This process is critically evident during type I hypersensitivity (allergic) reactions of the immune system for which mast cells are most commonly recognized. However, exocytosis of granular contents is fundamental to many mast cell functions, both allergic and nonallergic, and is a good indicator of mast cell activity. For example, whole blood levels of histamine and tryptase, both derived primarily from mast cell granules, are

often used as markers of mast cell activity.^{23–26} Regardless of the context, mast cell degranulation occurs when the intracellular signaling initiated by an external stimulus induces an increase in cytosolic calcium, triggering fusion of preformed dense body granules with the cell membrane. Table 1 lists several of the immunoreactive mediators released from mast cell granules *via* exocytosis. In this work, serotonin is of particular importance because of its electrochemical properties. The ability to measure serotonin release electrochemically offers a unique handle on the kinetic and mechanistic character of mast cell degranulation, providing a label-free way to monitor the release of many mast-cell-secreted mediators in a variety of physiological scenarios.

SCD is characterized by a single Glu-Val point mutation of the gene that encodes the β -subunit of Hb,² The mutation causes Hb to rapidly polymerize under hypoxic conditions,²⁷ and the accumulation of polymerized sickle Hb in deoxygenated red blood cells ultimately results in a variety of damaging physiological consequences.^{3,5} These include impaired rheological function of red blood cells, anemia, poor oxygenation of tissues, and intermittent vascular occlusion events, which are painful and contribute to organ failure.^{3,6} Although vascular occlusion is traditionally implicated as the primary cause of symptoms in SCD patients, underlying inflammation has become recognized as an important contributor to the disease.^{6,28–30} Inflammation initiated through oxidative stress and blood cell–endothelium interactions during vascular occlusive events is sustained in sickle cell patients and proliferates SCD symptoms.^{5,29,31} Despite their capacity to influence the immune response, the specific way mast cells function in various inflammatory environments has yet to be extensively explored. Given the chronic state of inflammation in SCD and the integral role of mast cells in many

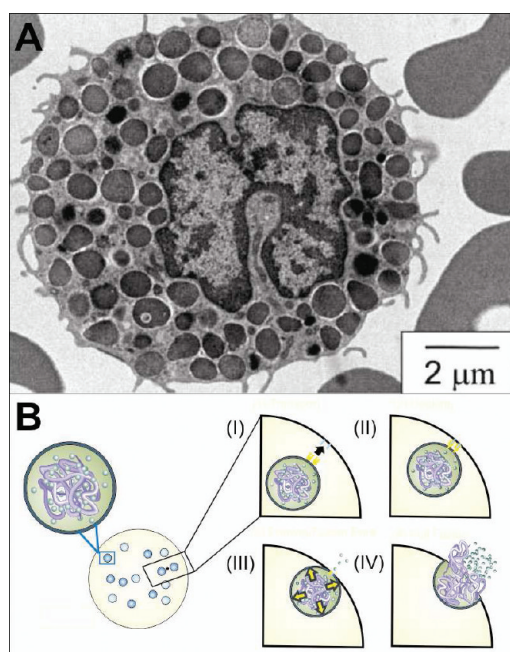


Figure 2. TEM image of a mast cell (A) clearly shows the dense-body granules that contain many biologically active mediators that influence the immune response. Once stimulated, mast cells release these mediators through exocytosis (B), during which individual granules are trafficked to the cell membrane where they dock with specialized proteins that help regulate the fusion of the granular and cell membranes and the subsequent release of the granular contents to the extracellular space. Exocytosis schematic (B) reprinted with permission of Kim, D., Köseoglu, S., Manning, B. M., Meyer, A. F., and Haynes, C. L. (2011) Electroanalytical eavesdropping on single cell communication. *Anal. Chem.* 83, 7242–7249. Copyright 2011 American Chemical Society.

Table 1. Granule-Associated Mediators^a

| Granule-associated Mediators | Examples of Function |
|----------------------------------------------------------|-------------------------------------------------------------|
| Histamine and serotonin | Alter vascular permeability |
| Heparin and/or chondroitin sulfate peptidoglycans | Enhance chemokine and/or cytokine function and angiogenesis |
| Tryptase, chymase, carboxypeptidase, and other proteases | Remodel tissue and recruit effector cells |
| TNF, VEGF, and FGF2 | Recruit effector cells and enhance angiogenesis |

^aMast cell granules contain several biologically active mediators that influence the immune response. Of these, only serotonin is electroactive at the applied potential. Table adapted from Marshall *et al.*²²

aspects of the immune system, it is critical to explore how mast cells contribute to the development and progression of this disease. Furthermore, because mast cells express opioid receptors and morphine is widely used to treat pain in SCD, it is pertinent to fully understand how morphine effects mast

cell function, both in general and in the context of chronic inflammation.

To better understand the nature of inflammation in SCD and the impact of morphine therapy on mast cells, CFMA was used to monitor the degranulation dynamics of mast cells isolated from two transgenic mouse models, one hemizygous (hBERK) and one homozygous (BERK) for human sickle Hb.^{16,32} As a control, mast cells from transgenic mice expressing normal human Hb (HbA-BERK) were used.³² All three mice were subject to treatment with either morphine or phosphate-buffered saline (PBS). Mast cell degranulation was monitored using CFMA, offering insight on (1) the change in mast cell function in the presence of SCD-associated inflammation, (2) the effect of morphine on control mast cells alone, and (3) how morphine treatment influences mast cell function in the presence of inflammation. Our results indicate mast cell function is significantly altered in transgenic mice expressing human sickle Hb through a complex mechanism regulating the exocytosis of stored mediators. Furthermore, in addition to its analgesic effects, this work suggests treatment with morphine may have implications for the state of inflammation in SCD. Ultimately, this work highlights the unique capacity of CFMA to address critical questions relating to mast cell biology and fundamental processes of inflammation.

RESULTS AND DISCUSSION

CFMA measurements were conducted on peritoneal mast cells isolated from HbA-BERK, hBERK1, and BERK mice following 3 weeks of morphine treatment (PBS was used for control conditions). Measurement from an individual cell produced a current trace consisting of a collection of current spikes each corresponding to an individual degranulation event. The focus of this work was to explore the role of mast cells in SCD and the influence of morphine on mast cell function, both alone and in the context of chronic inflammation as modeled by the hBERK1 and BERK transgenic mice. Single mast cells were stimulated locally with the calcium ionophore A23187, which was selected as a universal mast cell stimulant that would limit bias toward a specific activation pathway. For the purpose of fulfilling these aims, four characteristics of the CFMA traces, plotted as time versus current, were analyzed among the experimental conditions: spike area (Q), spike frequency, spike half-width ($t_{1/2}$), and spike rise-time (t_{rise}) (Figure 1E). Each spike characteristic reports on a different element of the exocytosis process. Analyzing the perturbations in several spike characteristics between experimental conditions provides a unique description of the mechanisms regulating the observed change in mast cell function.

Spike area (Q), the integral of each individual current spike over time, is a measure of charge and thus represents the number of electrons transferred per release event. Because the oxidation of serotonin is a two-electron process, the area of an individual spike can be converted to the number of serotonin molecules released per granule. Spike frequency is calculated as the number of release events detected over the total release time and corresponds to the efficiency of the overall granule transport, docking and fusion mechanisms. Together, total Q and spike frequency can be combined to reveal the amount of serotonin released per cell (taking into account that the microelectrode covers only ~10% of the cell surface area and assuming equal secretion from all regions of the cell). In addition to spike area and frequency, spike rise-time (t_{rise}) and half-width ($t_{1/2}$) values are monitored as a measure of the

serotonin release kinetics from each granule fusion event. The value of t_{rise} is calculated as the time between 10% and 90% of the full spike height on the rising phase of each current spike; t_{rise} reflects the amount of serotonin not directly associated with the chondroitin sulfate biopolymer matrix. Upon fusion, this “free” serotonin diffuses to the electrode surface more rapidly than the bulk of the intragranular serotonin that interacts strongly with the negatively charged matrix. The value of t_{rise} is heavily influenced by the dilation of the initially formed fusion pore (between the granule and the plasma membrane) to the maximally fused state. The value of $t_{1/2}$, the width of the spike at half its full height, is a measure of the rate by which the biopolymer matrix expands and unfolds, releasing the remaining matrix-associated serotonin. Together, $t_{1/2}$ and t_{rise} reflect the biophysical forces that determine the peak shape (sharp leading edge followed by a slower decay) typical of exocytotic release events.³³

To establish the impact of SCD-associated inflammation on mast cell function, mast cells isolated from PBS-treated HbA-BERK controls were compared to those from both hBERK1 and BERK mice (Figure 3A–C). The hBERK1 and BERK

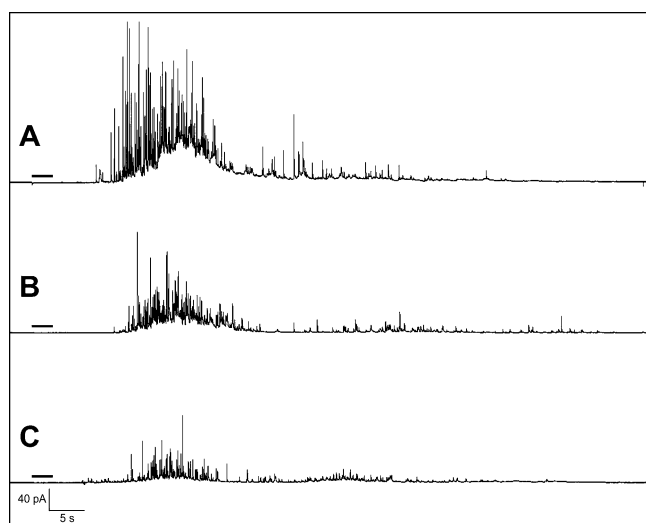


Figure 3. Representative current traces collected using CFMA to analyze degranulation behavior of mast cells isolated from HbA-BERK (A), hBERK1 (B), and BERK (C) mice in the absence of morphine treatment. Mast cells were stimulated locally with a 3 s bolus of 10 μM A23187.

conditions demonstrated 27% and 58% reductions in Q , respectively (Figure 4A). Although this effect was significant in only the BERK mouse, the observed decrease trends with increasing sickle Hb expression. In addition, both hBERK1 and BERK mast cells released their granular contents less efficiently, resulting in significantly decreased spike frequencies by 34% and 32%, respectively (Figure 4B). When considered in concert versus HbA-BERK controls over the course of a 30 s release, these two effects resulted in a modest, though not statistically significant, decrease in overall serotonin release of 37% (1.97×10^9 fewer molecules per cell) for hBERK1 mast cells and a greater, significant decrease of 72% (3.84×10^9 fewer molecules per cell) in the BERK condition. These data suggest that the chronic inflammation in SCD induces mast cells to release less serotonin per exocytotic event as a result of either decreased granule loading or decreased percent serotonin released per granule, as regulated by a reduction in secretion driving forces.

The relative magnitude of this effect appears to be dependent on disease severity. The reduced frequency of individual release events observed in both hBERK1 and BERK mast cells likely result from a decrease in either granule trafficking or fusion efficiency. Granule trafficking effects often occur due to perturbations of the microtubule transport machinery, whereas fusion efficiency is affected by changes in membrane stability. Unlike the observed changes in Q , changes in spike frequency observed in hBERK1 and BERK mice appear to be independent of disease severity.

Considering the observed sickle Hb-induced decrease in the number of secreted serotonin molecules (as indicated by Q), it is expected that, in the absence of changed release kinetics, $t_{1/2}$ would decrease because it should take less time to release a smaller amount of serotonin. However, mast cells from both hBERK1 and BERK mice demonstrated significantly larger $t_{1/2}$ values compared to those from the control mice (Figure 4C). Similarly, t_{rise} values increased by 79% and 39%, respectively, for hBERK1 and BERK mast cells compared to values for HbA-BERK controls (Figure 4D). This effect is also counter to the expected decrease resulting from the smaller Q values observed for both hBERK1 and BERK mice, with hBERK1 demonstrating the greatest increases in both $t_{1/2}$ and t_{rise} due to the smaller decreases in Q compared to BERK mast cells. It has been shown in other granulated cell types that individual exocytosis events do not release the full mediator content of each granule.⁹ Although serotonin loading effects cannot be ruled out entirely, the increase in $t_{1/2}$ and t_{rise} measured herein despite corresponding decreases in Q for both hBERK1 and BERK mast cells suggests a mechanism of decreased serotonin released per granule rather than a decrease in overall granule loading.

Together, the observed decreases in Q and spike frequency, in addition to the somewhat counterintuitive increases in both $t_{1/2}$ and t_{rise} , suggest that the chronic inflammation present in both hBERK1 and BERK mice modulates mast cell serotonin secretion through a multifaceted mechanism involving both the serotonin release efficiency as well as membrane driving forces that alter granule fusion. Although the decrease in serotonin released (as indicated by decreased Q values) appears to be controlled in part by both decreased rate of transition from fusion pore to “full” fusion (as indicated by increased t_{rise} values) and slower biopolymer matrix unfolding (as indicated by decreased $t_{1/2}$ values) rather than decreased serotonin storage, further research will be required to fully clarify the mechanism of this process. Similarly, the frequency effects observed in hBERK1 and BERK mast cells may also result from the same decreased membrane driving forces. The combination of changes in Q , spike frequency, $t_{1/2}$, and t_{rise} observed in mast cells from hBERK1 and BERK mice indicate the serotonin release process in SCD is modulated by multiple compounding mechanisms.

To explore the effect of chronic morphine treatment on mast cell function independent of the inflammation associated with SCD, the serotonin release dynamics of mast cells isolated from HbA-BERK mice treated with either morphine or PBS were analyzed. On average, mast cells from morphine-treated mice released 172% more serotonin per granule than those from PBS-treated controls with no significant change in frequency (Figure 5A,B). When the effects of Q and spike frequency are combined as a measure of total serotonin released, a 162% increase in overall serotonin released per cell is observed, corresponding to 8.66×10^9 more serotonin molecules, and is

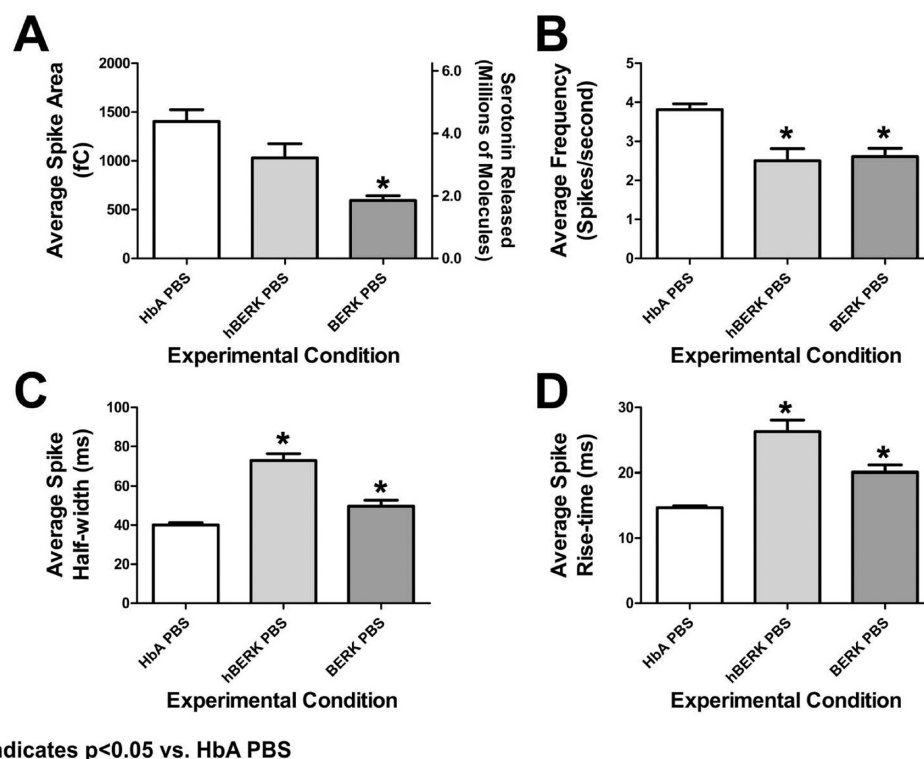


Figure 4. Effect of sickle Hb expression and the corresponding chronic inflammation on mast cell function explored using CFMA. Mast cells from PBS-treated HbA-BERK ($n = 77$), hBERK1 ($n = 28$), and BERK ($n = 30$) mast cells were analyzed by CFMA. Spike area (A), spike frequency (B), spike half-width (C), and spike rise-time (D) were compared. Statistical significance was determined using the two-tailed Student's t test. Mast cells were stimulated locally with a 3 s bolus of $10 \mu\text{M}$ A23187.

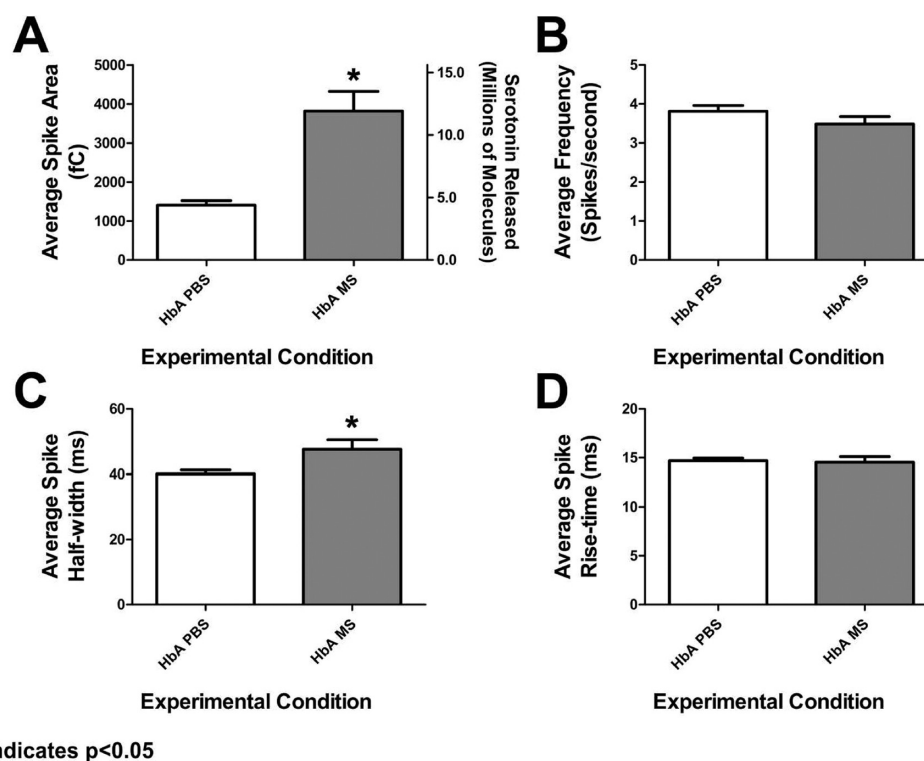


Figure 5. Effect of chronic morphine (MS) treatment on mast cells in the absence of chronic inflammation. Mast cells from HbA-BERK mice treated with either PBS ($n = 77$) or morphine ($n = 47$) were analyzed by CFMA. Spike area (A), spike frequency (B), spike half-width (C), and spike rise-time (D) were monitored and analyzed for statistical significance using the two-tailed Student's t test. Mast cells were stimulated locally with a 3 s bolus of $10 \mu\text{M}$ A23187.

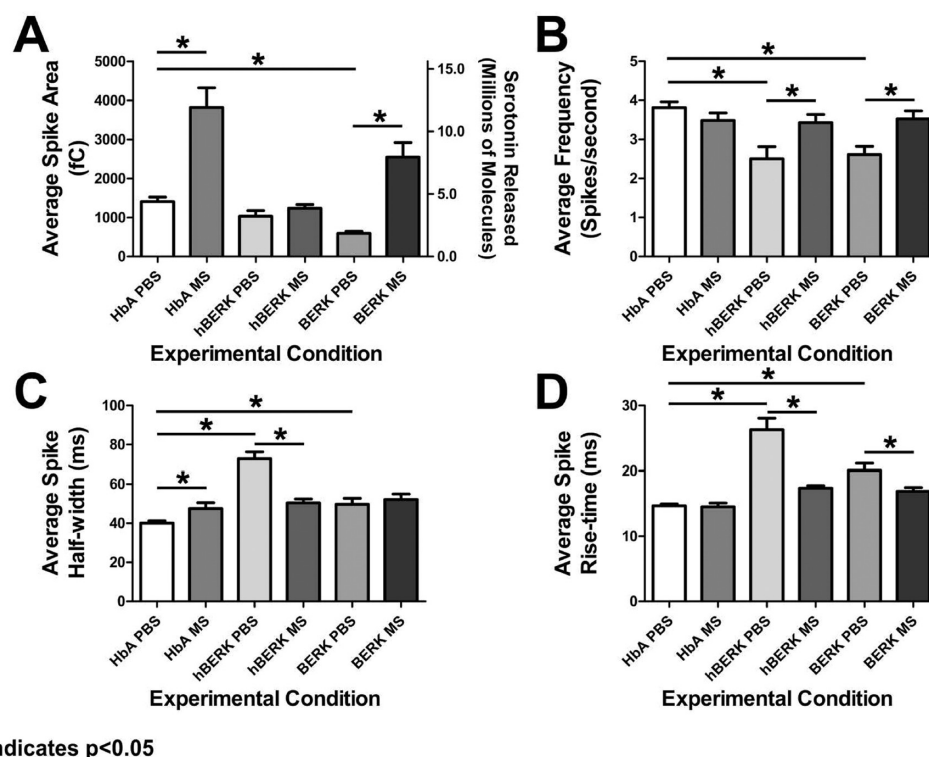


Figure 6. Effect of morphine on mast cell function in sickle cell mice. Mast cells from MS-treated HbA-BERK ($n = 47$), hBERK ($n = 52$), and HbA-BERK ($n = 47$) mice were compared to PBS-treated controls ($n = 77$ for HbA-BERK, $n = 28$ for hBERK, $n = 30$ for BERK) and analyzed using CFMA. Spike area (A), spike frequency (B), spike half-width (C), and spike rise-time (D) were monitored and analyzed for statistical significance using the two-tailed Student's t test. Mast cells were stimulated locally with a 3 s bolus of 10 μ M A23187.

entirely due to increased serotonin released per granule. Interestingly, chronic morphine exposure resulted in a small, significant increase in $t_{1/2}$ (19%), which is expected considering the large observed increase in Q (Figure 5C). This expected result reflects the inherent association between $t_{1/2}$ and Q . Other explanations for this $t_{1/2}$ increase require invocation of an unnecessarily complex regulatory mechanism. No morphine-induced increase in t_{rise} was observed for mast cells from HbA-BERK mice (Figure 5D).

Unlike the complex disease-induced change in mast cell function described above, the observed effect of morphine treatment on mast cells in HbA-BERK mice appears to originate from a simpler mechanism. The large morphine-induced increase in serotonin released per granule is not associated with changes in the monitored spike parameters other than Q . These data suggest morphine treatment induces mast cells to either store more serotonin per granule or release a greater portion of its granular contents per release event. The lack of unexpected changes in $t_{1/2}$ or t_{rise} suggest that the driving forces of granule fusion are not markedly altered by chronic morphine exposure in mast cells from HbA-BERK mice. Therefore, increased serotonin loading is more likely responsible for the large increase in serotonin released per granule from these mast cells.

Finally, the effect of chronic morphine treatment on hBERK1- and BERK-derived mast cells was investigated. With respect to the effect on serotonin released per granule, mast cells from BERK mice demonstrated significantly increased Q values sufficient to more than recover the 58% reduction in Q attributed to the expression of sickle Hb (Figure 6A). Although statistically insignificant, a smaller recovery trend was also seen in hBERK1-derived mast cells (Figure 6A).

Interestingly, although in HbA-BERK mice morphine had no effect on release frequency, mast cells from both hBERK1 and BERK mice responded to morphine treatment by reversing the depressed frequencies observed for the PBS conditions in each (Figure 6B). In addition, treatment with morphine significantly recovered the sickle Hb-induced increases in t_{rise} in mast cells from both hBERK1 and BERK mice (Figure 6D). A similarly significant recovery effect was observed in the $t_{1/2}$ values in the hBERK1 condition (Figure 6C), and although a morphine-induced recovery of the $t_{1/2}$ values was not observed for the BERK condition, this is attributable to the relatively smaller initial sickle Hb-induced effect in these mice (Figure 6C).

Given the large morphine-induced increase in Q in mast cells from HbA-BERK control mice, the observed recovery of Q in BERK mice, although important, is perhaps less surprising compared to the morphine-induced recoveries observed for spike frequency, t_{rise} , and $t_{1/2}$ despite the lack of morphine-mediated effects on any of these parameters in the HbA-BERK mice (with the exception of $t_{1/2}$ values in the HbA-BERK mice as mentioned above). For all measured parameters, it is worth noting that the morphine-induced recoveries that were observed did not grossly exceed the corresponding values measured from morphine treated HbA-BERK controls (Figure 6). Interestingly, Q was the only measured parameter demonstrating overcompensation behavior in response to treatment with morphine (relative to mast cells from PBS-treated HbA-BERK mice). Nonetheless, Q values in morphine-treated hBERK1 or BERK mice did not exceed those from morphine-treated HbA-BERK mice (Figure 6A). It is likely that the increased amount of serotonin released from mast cells from morphine-treated hBERK1 and BERK mice (as demonstrated by an increase in Q) results from a combination

of granule loading and increased granule fusion driving forces. Because granule loading was found to be the sole observed mechanism of morphine-mediated regulation of serotonin release in HbA-BERK mast cells, these data indicate that the morphine-induced increase in serotonin loading is independent of inflammation. In contrast, this data suggests the ability of morphine to recover mast cell functionality *via* regulation of matrix unfolding and membrane driving forces (the mechanisms likely responsible for decreasing the amount of serotonin released from mast cells in hBERK1 and BERK mice) as measured by spike frequency, t_{rise} and $t_{1/2}$, may be limited to levels similar to morphine-treated controls. According to this hypothesis, these findings argue matrix unfolding effects and membrane driving forces are rate limited under normal conditions, resulting in minimal perturbation of these factors in non-SCD mice upon morphine exposure.

To summarize, this research proposes that chronic inflammation in mice expressing human sickle Hb impairs the secretion of serotonin from mast cells through multiple mechanisms, including fusion pore formation/modulated membrane driving forces and matrix expansion efficiency. Chronic morphine treatment was found to act differently on mast cells from non-sickle cell mice (HbA-BERK) than those expressing human sickle Hb (hBERK1 and BERK). In the absence of SCD-associated inflammation, morphine exposure induced mast cells to increase the amount of serotonin released per granule, a relatively simple mechanism likely resulting from increased serotonin loading. However, morphine treatment induced a more complex change in mast cells isolated from hBERK1 and BERK mice. Whereas only serotonin loading effects were observed in mast cells from HbA-BERK mice, morphine induced marked recovery of all the sickle-cell-induced perturbations in mast cell function in both hBERK1 and BERK mice. Morphine was observed to both increase serotonin loading and restore membrane driving forces to levels similar to those of morphine-treated control mice. Given the capacity for mast cells to influence the inflammatory micro-environment and the importance of inflammation in the progression of SCD, these findings offer unique insight into (1) the significantly altered mast cell function in response to sickle-cell-induced inflammation, (2) the large morphine-induced increase in serotonin released per mast cell, and (3) the capacity for morphine to compensate for sickle-cell-induced changes in mast cell function.

Any broad-reaching implications of these findings will require significant additional research to characterize both the extent to which mast cells influence the chronic inflammation in SCD as well as the relative importance of morphine in regulating mast cell function when considering available treatment options. Furthermore, in light of tissue-specific mast cell heterogeneity, further work is required to evaluate the universality of these findings. However, it is clear from this study that mast cell function is indeed altered in mice expressing sickle Hb. It is apparent that the use of morphine to treat the pain associated with SCD may also influence the inflammatory state of the disease. Deciphering the root cause of sickle Hb-induced mast cell effects and determining whether morphine complicates or improves the pathophysiology of SCD, and the extent of either, will be the subject of future collaborative research in this area.

METHODS

In Vivo Morphine Treatment. All mice were bred in a germ-free AAALAC accredited animal facility at the University of Minnesota as

described previously.¹⁶ Each mouse was genotyped and phenotyped for the expression of human sickle hemoglobin. All animal experiments were performed after Institutional approvals. BERK mice used herein are homozygous for knockout of murine α and β globins and express human sickle hemoglobin (β^S globins). These mice express ~99% human sickle hemoglobin.³² hBERK1 mice are homozygous for knockout of α globin but hemizygous for β globin. These mice express a single transgene for human α and β^S hemoglobin. Both BERK and hBERK1 mice are on a mixed genetic background. Therefore, mice on a similar mixed genetic background, HbA-BERK expressing human α and normal human hemoglobin (β^A globin), were used as control.

HbA-BERK, hBERK1, and BERK mice were injected subcutaneously with morphine twice daily at doses of 0.75 mg/kg/day the first week, 1.4 mg/kg/day the second week, and 2.14 mg/kg/day the final week. Each dose of morphine was delivered in 50 μ L of phosphate-buffered saline (PBS) (Invitrogen). Following the third week of exposure, mice were euthanized by CO₂ asphyxiation for mast cell isolation by peritoneal lavage.

Due to the low-throughput nature of single cell measurements, three week *in vivo* exposure protocols were staggered to allow CFMA experiments to be conducted on six days over the course of three weeks. Measurements from PBS-treated HbA-BERK control mast cells were made in parallel on each day to ensure consistency across all CFMA conditions. One day's worth of experiments were thrown out due to average spike area values exceeding 1.5 standard deviations from the comprehensive mean of PBS-treated HbA-BERK controls, over three times larger than the deviations of the other control data sets.

Cell Culture. Mouse 3T3 fibroblasts were maintained continuously in lab as described previously.¹¹ Primary mouse peritoneal mast cells were collected using methods previously described.^{11,34} In brief, mice were euthanized by CO₂ asphyxiation in accordance with IACUC Protocol 0806A37663 (PI Gupta K; Title: "Opioid activity in endothelium in SCD"). The peritoneal cavity of each mouse was then injected with about 8 mL of cold DMEM high glucose media supplemented with 10% (v/v) BCS and 1% penicillin/streptomycin. After 20–30 s of massage, the media was extracted and stored on ice. The collected media was centrifuged for 5 min at 400 \times g, and the cell pellet was dispersed in fresh media and plated onto confluent mouse 3T3 fibroblasts previously grown to confluence in 35 \times 10 mm Petri dishes. Mast cells were incubated at 37 °C for 24 h prior to measurement by CFMA.

Microelectrode Fabrication. Carbon-fiber microelectrodes were fabricated in lab following the previously described procedure.^{11,35} Prior to use in CFMA experiments, microelectrodes were beveled to 45° on a diamond polishing wheel (Sutter Instruments) and stored in isopropyl alcohol. To ensure conductivity to the potentiostat headstage, electrodes were backfilled with an electrolyte solution (3.0 M potassium acetate, 30.0 mM potassium chloride) and mounted on a platinum-coated silver wire (Squires Electronics).

CFMA Measurements. Media was removed from the co-cultured mast cells before being washed and replaced with warm Tris buffer (12.5 mM tris(hydroxymethyl)aminomethane hydrochloride, 150 mM NaCl, 4.2 mM KCl, 5.6 mM glucose, 1.5 mM CaCl₂, 1.4 mM MgCl₂, sterile filtered and pH balanced to 7.2–7.4). The Petri dish was then placed in a plate warmer (Warner Instruments LLC) on an inverted microscope (Nikon). A polished and backfilled microelectrode was mounted onto a headstage connected to an Axon Instruments Axopatch 200B potentiostat (Molecular Devices Inc.) to permit control of the applied voltage. A pulled glass capillary micropipet was loaded with 10 μ M A23187 (Sigma Aldrich) and connected to a Picospritzer III (Parker Hannifin) for controlled delivery of the stimulating solution. Both the micropipet and the headstage-mounted microelectrode were mounted on Burleigh PCS-5000 piezoelectric micromanipulators (Olympus America Inc.). After lowering the microelectrode into solution, its potential was set to +700 mV versus a silver/silver chloride (Ag/AgCl) reference electrode. Immediately prior to data collection, the electrode was placed in contact with the cell membrane of a single mast cell, and the stimulating pipet was then placed in close proximity. Upon collection of the amperometric trace, a

3-s dose of 10 μ M A23187 was delivered, inducing the degranulation. Oxidizing currents corresponding to discrete release events were detected as a function of time.

Data Analysis and Statistics. Amperometric traces were collected using Tar Heel software (courtesy of Dr. Michael Heien) and processed at 200 Hz with a Bessel low-pass filter before spike parameter analysis using Minianalysis software (Synptosoft, Inc.). Average spike parameter values were obtained for each amperometric trace representing the exocytosis of granules from a single mast cell.³³

Within each condition, average spike parameter values from individual cells were statistically analyzed for outliers. The log of the average spike parameters was calculated for all amperometric traces of a given condition. These log averages were then averaged again, and a standard deviation was calculated. If a log value for a single amperometric trace fell outside two standard deviations of the average of averages for that spike parameter, the trace was discarded as an outlier for all monitored parameters. For example, if the average Q obtained from a single mast cell was found to be an outlier, the spike frequency, t_{rise} , and $t_{1/2}$ values corresponding to that same amperometric trace were also discarded. The log-biased statistical treatment was selected to offset the bias toward larger spikes that results from the data fitting process. After statistical analysis, experimental condition averages were calculated for each spike parameter.³⁶ The significance of differences between these values was determined using the two-tailed student's t test with 95% confidence used as the threshold for statistical significance.

AUTHOR INFORMATION

Corresponding Author

*E-mail: chaynes@umn.edu.

ACKNOWLEDGMENTS

The authors would like to thank B. Marquis, S. Love, M. Maurer-Jones, S. Koseoglu, A. Meyer, and D. Kim for their assistance during preliminary experiments. Technical assistance from J. Ngyuen with mouse experiments is appreciated. We would also like to thank R. M. Wightman for the SEM image in Figure 1A,B. Marquis and K. Braun for the mast cell image in Figure 2A, and S. Love for providing Figure 2B. This work is funded by the National Institutes of Health New Innovator Award 1 DP2 OD004258-01 to C.L.H., RO1 HL68802 and HL103773 to K.G., PO1 HL55552 to R.P.H., and the National Institutes of Health Chemistry Biology Interface Training Grant (GM 08700) to B.M.M.

REFERENCES

- (1) Pauling, L., Itano, H. A., Singer, S. J., and Wells, I. C. (1949) Sickle cell anemia, a molecular disease. *Science* 110, 543–548.
- (2) Ingram, V. M. (1957) Gene mutations in human haemoglobin: the chemical difference between normal and sickle cell haemoglobin. *Nature* 180, 326–328.
- (3) Frenette, P. S., and Atweh, G. F. (2007) Sickle cell disease: old discoveries, new concepts, and future promise. *J. Clin. Invest.* 117, 850–858.
- (4) Kaul, D. Sickle cell disease. *Compr. Physiol.* 2008, DOI: 10.1002/cphy.cp020417.
- (5) Kaul, D. (2009) Insights into vascular pathobiology of sickle cell disease. *Hematologie* 15, 446–457.
- (6) Conran, N., Franco-Penteado, C. F., and Costa, F. F. (2009) Newer aspects of the pathophysiology of sickle cell disease vaso-occlusion. *Hemoglobin* 33, 1–16.
- (7) Rees, D. C., Williams, T. N., and Gladwin, M. T. (2010) Sickle-cell disease. *Lancet* 376, 2018–2031.
- (8) Kita, J. M., and Wightman, R. M. (2008) Microelectrodes for studying neurobiology. *Curr. Opin. Chem Biol.* 12, 491–496.
- (9) Omiatsek, D. M., Dong, Y., Heien, M. L. A. V., and Ewing, A. G. (2010) Only a fraction of quantal content is released during exocytosis

as revealed by electrochemical cytometry of secretory vesicles. *ACS Chem. Neurosci.* 1, 234–245.

(10) Ge, S., Woo, E., White, J. G., and Haynes, C. L. (2011) Electrochemical measurement of endogenous serotonin release from human blood platelets. *Anal. Chem.* 83, 2598–2604.

(11) Marquis, B. J., McFarland, A. D., Braun, K. L., and Haynes, C. L. (2008) Dynamic measurement of altered chemical messenger secretion after cellular uptake of nanoparticles using carbon-fiber microelectrode amperometry. *Anal. Chem.* 80, 3431–3437.

(12) Kalesnikoff, J., and Galli, S. J. (2008) New developments in mast cell biology. *Nat. Immunol.* 9, 1215–1223.

(13) Moon, T. C., St Laurent, C. D., Morris, K. E., Marcet, C., Yoshimura, T., Sekar, Y., and Befus, A. D. (2010) Advances in mast cell biology: new understanding of heterogeneity and function. *Mucosal Immunol.* 3, 111–128.

(14) Kalesnikoff, J., and Galli, S. J. (2011) Antiinflammatory and immunosuppressive functions of mast cells. *Methods Mol. Biol.* 677, 207–220.

(15) Darbari, D. S., Minniti, C. P., Rana, S., and van den Anker, J. (2008) Pharmacogenetics of morphine: Potential implications in sickle cell disease. *Am. J. Hematol.* 83, 233–236.

(16) Kohli, D. R., Li, Y., Khasabov, S. G., Gupta, P., Kehl, L. J., Ericson, M. E., Nguyen, J., Gupta, V., Heibel, R. P., Simone, D. A., and Gupta, K. (2010) Pain-related behaviors and neurochemical alterations in mice expressing sickle hemoglobin: modulation by cannabinoids. *Blood* 116, 456–465.

(17) Darbari, D. S., Neely, M., van den Anker, J., and Rana, S. (2011) Increased clearance of morphine in sickle cell disease: implications for pain management. *J. Pain* 12, 531–538.

(18) Blunk, J., Schmelz, M., Zeck, S., Skov, P., and Likar, R. (2004) Opioid-induced mast cell activation and vascular responses is not mediated by μ -opioid receptors: An in vivo microdialysis study in human skin. *Anesth. Analg.* 98, 364–370.

(19) Klinker, J. F., and Seifert, R. (1997) Morphine and muscle relaxants are receptor-independent G-protein activators and cromolyn is an inhibitor of stimulated G-protein activity. *Inflammation Res.* 46, 46–50.

(20) Barke, K. E., and Hough, L. B. (1993) Opiates, mast cells and histamine release. *Life Sci.* 53, 1391–1399.

(21) Okayama, Y., and Kawakami, T. (2006) Development, migration, and survival of mast cells. *Immunol. Res.* 34, 97–115.

(22) Marshall, J. S. (2004) Mast-cell responses to pathogens. *Nat. Rev. Immunol.* 4, 787–799.

(23) Zdravkovic, V., Pantovic, S., Rosic, G., Tomic-Lucic, A., Zdravkovic, N., Colic, M., Obradovic, Z., and Rosic, M. (2011) Histamine blood concentration in ischemic heart disease patients. *J. Biomed. Biotechnol.* 2011, 1–8.

(24) Wojtecka-Lukasik, E., Ksiezopolska-Orlowska, K., Gaszewska, E., Krasowicz-Towalska, O., Rzodkiewicz, P., Maslinska, D., Szukiewicz, D., and Maslinski, S. (2010) Cryotherapy decreases histamine levels in the blood of patients with rheumatoid arthritis. *Inflamm. Res.* 59 (Suppl 2), S253–5.

(25) Schwartz, L. B., Irani, A. M., Roller, K., Castells, M. C., and Schechter, N. M. (1987) Quantitation of histamine, tryptase, and chymase in dispersed human T and TC mast cells. *J. Immunol.* 138, 2611–2615.

(26) Shore, P. A., Burkhalter, A., and Cohn, V. H. (1959) A method for the fluorometric assay of histamine in tissues. *J. Pharmacol. Exp. Ther.* 127, 182–186.

(27) Kaul, D. K., Fabry, M. E., Windisch, P., Baez, S., and Nagel, R. L. (1983) Erythrocytes in sickle cell anemia are heterogeneous in their rheological and hemodynamic characteristics. *J. Clin. Invest.* 72, 22–31.

(28) Hagar, W., and Vichinsky, E. (2008) Advances in clinical research in sickle cell disease. *Br. J. Haematol.* 141, 346–356.

(29) Conran, N., and Costa, F. F. (2009) Hemoglobin disorders and endothelial cell interactions. *Clin. Biochem.* 42, 1824–1838.

(30) Ballas, S. K. (2007) Current issues in sickle cell pain and its management. *Hematol. Am. Soc. Hematol. Educ. Program*, 97–105.

(31) Hebbel, R. P., Osarogiagbon, R., and Kaul, D. (2004) The endothelial biology of sickle cell disease: inflammation and a chronic vasculopathy. *Microcirculation* 11, 129–151.

(32) Paszty, C. (1997) Transgenic knockout mice with exclusively human sickle hemoglobin and sickle cell disease. *Science* 278, 876–878.

(33) Mosharov, E. V., and Sulzer, D. (2005) Analysis of exocytotic events recorded by amperometry. *Nat. Methods* 2, 651–658.

(34) Pihel, K., Hsieh, S., Jorgenson, J. W., and Wightman, R. M. (1995) Electrochemical detection of histamine and 5-hydroxytryptamine at isolated mast cells. *Anal. Chem.* 67, 4514–4521.

(35) Wightman, R. M., Jankowski, J. A., Kennedy, R. T., Kawagoe, K. T., Schroeder, T. J., Leszczyszyn, D. J., Near, J. A., Diliberto, E. J., and Viveros, O. H. (1991) Temporally resolved catecholamine spikes correspond to single vesicle release from individual chromaffin cells. *Proc. Natl. Acad. Sci. U.S.A.* 88, 10754–10758.

(36) Colliver, T. L., Hess, E. J., Pothos, E. N., Sulzer, D., and Ewing, A. G. (2000) Quantitative and statistical analysis of the shape of amperometric spikes recorded from two populations of cells. *J. Neurochem.* 74, 1086–1097.